Contents lists available at ScienceDirect

Physics Letters B

journal homepage: www.elsevier.com/locate/physletb

System-size dependence of the charged-particle pseudorapidity density at $\sqrt{s_{\mathrm{NN}}} = 5.02\,\mathrm{TeV}$ for pp, p–Pb, and Pb–Pb collisions

ALICE Collaboration ⋆

A R T I C L E I N F O

Article history:
Received 20 May 2022
Received in revised form 17 January 2023
Accepted 17 January 2023
Available online xxxx
Editor: M. Doser

A B S T R A C T

We present the first systematic comparison of the charged-particle pseudorapidity densities for three widely different collision systems, pp, p–Pb, and Pb–Pb, at the top energy of the Large Hadron Collider ($\sqrt{s_{\mathrm{NN}}} = 5.02\,\mathrm{TeV}$) measured over a wide pseudorapidity range ($-3.5 < \eta < 5$), the widest possible among the four experiments at that facility. The systematic uncertainties are minimised since the measurements are recorded by the same experimental apparatus (ALICE). The distributions for p–Pb and Pb–Pb collisions are determined as a function of the centrality of the collisions, while results from pp collisions are reported for inelastic events with at least one charged particle at midrapidity. The charged-particle pseudorapidity densities are, under simple and robust assumptions, transformed to charged-particle rapidity densities. This allows for the calculation and the presentation of the evolution of the width of the rapidity distributions and of a lower bound on the Bjorken energy density, as a function of the number of participants in all three collision systems. We find a decreasing width of the particle production, and roughly a smooth ten fold increase in the energy density, as the system size grows, which is consistent with a gradually higher dense phase of matter.

1. Introduction

The number of charged particles produced in energetic nuclear collisions is an important indicator for the strong interaction processes that determine the particle production at the sub-nucleonic level. In particular, the production of charged particles is expected to reflect the number of quark and gluon collisions occurring during the initial stages of the reaction. The total number of particles produced also provides information on the energy transfer available from the initial colliding beams to particle production, as a consequence of nuclear stopping [1]. In order to help unravel this complex scenario it is important to compare the particle production amongst collision systems of different sizes over a wide kinematic range.

We present the measured charged-particle pseudorapidity density, $\mathrm{d}N_{\mathrm{ch}}/\mathrm{d}\eta$, for pp, p–Pb, and Pb–Pb (previously published [2]) collisions at the same collision energy of $\sqrt{s_{\mathrm{NN}}} = 5.02\,\mathrm{TeV}$ in the nucleon–nucleon centre-of-mass reference frame. This is, at present, the maximum available energy at CERN's Large Hadron Collider (LHC) for Pb–Pb collisions. The measurements were carried out using ALICE at LHC (for earlier $\mathrm{d}N_{\mathrm{ch}}/\mathrm{d}\eta$ results see for example Refs. [3–5]). The three studied reactions have different characteristics probing widely different particle production yields and mechanisms. In Pb–Pb collisions, the total particle yield for central collisions is of the order 10^4 [2], and a strongly coupled plasma of quarks and gluons (sQGP) is formed [6–9], whose collective and transport properties are currently under intense study. On the other hand, pp collisions represent the simplest possible nuclear collision system, where the average total particle production is much smaller (≈80, by integrating the measured distributions), and is to first approximation much less subject to collective effects [10]. The p–Pb system is intermediate to the other reactions, corresponding to the situation where a single nucleon probes the nucleons in a narrow cylinder of the target nucleus. The extent to which p–Pb is governed by the initial state cold nuclear matter of the lead ion or whether collective phenomena in the hot and dense medium play an important role is, at present, a matter under scrutiny by the community [10,11].

In this letter, we compare the three reactions and present the ratios of the charged-particle pseudorapidity density distributions ($\mathrm{d}N_{\mathrm{ch}}/\mathrm{d}\eta$) of the more complex reactions to the pp distribution. Owing to ALICE's unique large acceptance in pseudorapidity, and using simple and robust assumptions, we transform the measured charged-particle pseudorapidity density distributions into charged-particle rapidity density distributions ($\mathrm{d}N_{\mathrm{ch}}/\mathrm{d}y$). This allows us to calculate the width of the rapidity distributions as a function of the number of participating nucleons. The parameters of the

⋆ *E-mail address:* alice-publications@cern.ch.

https://doi.org/10.1016/j.physletb.2023.137730
0370-2693/

transformation also allow us to estimate a lower bound on the energy density using the well-known formula from Bjorken [12]. An energy density exceeding the critical energy density of roughly $1\,\mathrm{GeV/fm^3}$ [13] is a necessary condition for the formation of deconfined matter of quarks and gluons, and thus it is of the utmost interest to understand the development of these energy densities across different collision systems.

2. Experimental set-up, data sample, analysis method, systematic uncertainties

A detailed description of the ALICE detector and its performance can be found elsewhere [14,15]. The present analysis uses the Silicon Pixel Detector (SPD) to determine the pseudorapidity densities in the range $-2 < \eta < 2$ and the Forward Multiplicity Detector (FMD) in the ranges $-3.5 < \eta < -1.8$ and $1.8 < \eta < 5$. The V0, comprised of two plastic scintillator discs covering $-3.7 < \eta < -1.7$ (V0C) and $2.8 < \eta < 5.1$ (V0A), and the ZDC, two zero-degree calorimeters located 112.5 m from the interaction point, measurements determine the collision centrality and are used for offline event selection [2].

The results presented are based on data from collisions at a centre-of-mass energy per nucleon pair of $\sqrt{s_{\mathrm{NN}}} = 5.02\,\mathrm{TeV}$ as collected by ALICE during LHC Run 1 (2013) for p–Pb, and during Run 2 (2015) for pp and Pb–Pb. The FMD suffered high levels of background noise during the 2016 p–Pb campaign, due to the high collision rate, and this data is therefore not used for the present analysis. About 10^5 events with a minimum bias trigger requirement [2] were analysed in the centrality range from 0% to 90% and 0% to 100% of the visible cross section for Pb–Pb and p–Pb collisions, respectively. The minimum bias trigger for p–Pb and Pb–Pb collisions in ALICE was defined as a coincidence between the V0A and V0C sides of the V0 detector.

The data from the p–Pb collisions were taken in two beam configurations: one where the lead ion travelled toward positive pseudorapidity and one where it travelled toward negative pseudorapidity. The results from the latter collisions are mirrored around $\eta = 0$. The centre-of-mass frame in p–Pb collisions does not coincide with the laboratory frame, due to the single magnetic field in the LHC, and thus the rapidity of the centre-of-mass is $y_{\mathrm{CM}} = \pm 0.465$ for the two directions, respectively, in the laboratory frame. For this reason, pseudorapidity, calculated with respect to the laboratory frame, is denoted η_{lab} whenever p–Pb results are presented.

Likewise, for the pp collisions, about 10^5 events with coincidence between V0A and V0C and at least one charged particle in $|\eta| < 1$ were analysed. By requiring at least one charged particle at midrapidity, the so-called INEL>0 event class, the systematic uncertainty, related to the absolute normalisation to the full inelastic cross section, is reduced, while still sampling a large fraction ($> 75\%$) of the hadronic cross section [16,17].

The standard ALICE event selection [18] and centrality estimator based on the V0 amplitude [19,20] are used in this analysis. The event selection consists of: a) exclusion of background events using the timing information from the ZDC (for Pb–Pb and p–Pb, e.g., beam–gas interactions) and V0 detectors, b) verification of the trigger conditions, and c) a reconstructed position of the collision (primary vertex). In Pb–Pb collisions, centrality is obtained from the sum amplitude in both V0 detector arrays (V0M). For p–Pb only the amplitude in the array on the lead-going side (V0A or V0C) is used. In Pb–Pb collisions, the 10% most peripheral collisions have substantial contributions from electromagnetic processes and are therefore not included in the results presented here [19].

A primary charged particle is defined as a charged particle with a mean proper lifetime τ larger than 1 cm/c, which is either a) produced directly in the interaction, or b) from decays of particles with τ smaller than 1 cm/c [21]. All quantities reported here are for primary, charged particles, though "primary" is omitted in the following for brevity.

The analysis method is identical to that of previous publications [2]: the measurement of the charged-particle pseudorapidity density at midrapidity is obtained from counting particle trajectories determined using the two layers of the SPD. The SPD has a lower transverse momentum acceptance of $50\,\mathrm{MeV}/c$, and the yield is extrapolated down to $p_{\mathrm{T}} = 0\,\mathrm{MeV}/c$ via simulations. In the forward regions, the measurement is provided by the analysis of the deposited energy signal in the FMD and a statistical method is employed to calculate the inclusive number of charged particles. A data-driven correction [22], based on separate measurements exploiting displaced collision vertices, is applied to remove the background from secondary particles.

Systematic uncertainty estimations for the midrapidity measurements are detailed elsewhere [2,16,20], and are from background suppression, transverse momentum extrapolation, weak decays, and simulations. The estimates are obtained through variation of thresholds and simulation studies. For pp (p–Pb), the total systematic uncertainty amounts to 1.5% (2.7%) over the whole pseudorapidity range; while for Pb–Pb the total systematic uncertainty is 2.6% at $\eta = 0$ and 2.9% at $|\eta| = 2$. The systematic uncertainty is mostly correlated over pseudorapidity for $|\eta| < 2$, and largely independent of centrality. The uncertainty in the forward region, estimated via variations of thresholds and simulation studies, is the same for all collision systems and is uncorrelated across η, amounting to 6.9% for $\eta > 3.5$ and 6.4% elsewhere within the forward regions [22]. In the figures of this letter, uncorrelated, local in pseudorapidity, systematic uncertainties are indicated by open boxes on the data points, while correlated systematic uncertainties, those that affect the overall scale and typically from event classification and selection, are indicated by filled boxes to the right of the data. The systematic uncertainty on $\mathrm{d}N_{\mathrm{ch}}/\mathrm{d}\eta$, due to the centrality class definition in Pb–Pb, is estimated to vary from 0.6% for the most central to 9.5% for the most peripheral class [23]. The 80% to 90% centrality class has residual contamination from electromagnetic processes as detailed elsewhere [19], which gives rise to an additional 4% systematic uncertainty in the measurements. No overall systematic uncertainty has been estimated for p–Pb collisions, as the centrality selection in that collision system is inherently difficult to map to the underlying dynamics of the collisions [20].

3. Results

Fig. 1 shows the measured pseudorapidity densities in pp, and in central p–Pb, and the previously published results for Pb–Pb [2] collisions at $\sqrt{s_{\mathrm{NN}}} = 5.02\,\mathrm{TeV}$ for primary particles.

For the 5% most central Pb–Pb collisions $\mathrm{d}N_{\mathrm{ch}}/\mathrm{d}\eta \approx 2000$ at midrapidity ($\eta = 0$) [2], while for p–Pb collisions the distribution peaks at $\mathrm{d}N_{\mathrm{ch}}/\mathrm{d}\eta_{\mathrm{lab}} \approx 60$ around $\eta_{\mathrm{lab}} = 3$ in the lead-going direction ($\eta > 0$). For pp collisions with the INEL>0 trigger condition discussed above, $\mathrm{d}N_{\mathrm{ch}}/\mathrm{d}\eta = 5.7 \pm 0.2$ at midrapidity, consistent with previous results derived from p_{T} spectra [24].

Fig. 2 shows, as a function of centrality, the measured charged-particle pseudorapidity densities for p–Pb collisions at $\sqrt{s_{\mathrm{NN}}} = 5.02\,\mathrm{TeV}$. The strategy of centrality selection for proton on nucleus reactions is explained elsewhere [20]. The ALICE Collaboration has previously presented $\mathrm{d}N_{\mathrm{ch}}/\mathrm{d}\eta$ for Pb–Pb collisions at this energy [2].

In Fig. 3, the charged-particle pseudorapidity densities in p–Pb and Pb–Pb reactions are divided by the pp distributions corresponding to the INEL>0 trigger class. The ratio is $r_X = (\mathrm{d}N_{\mathrm{ch}}/\mathrm{d}\eta|_X)/(\mathrm{d}N_{\mathrm{ch}}/\mathrm{d}\eta|_{\mathrm{pp}})$, where X labels p–Pb and Pb–Pb collisions, in centrality classes, as a function of pseudorapidity. In

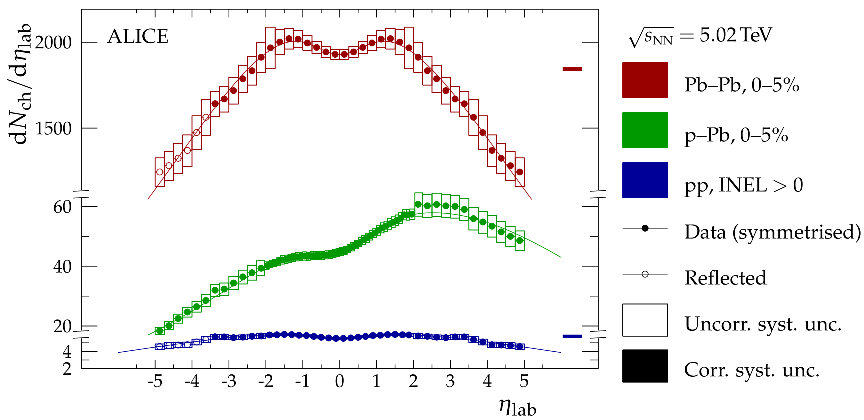

Fig. 1. Charged-particle pseudorapidity density in Pb–Pb [2] and p–Pb for the 5% most central collisions, and for pp collisions with INEL>0 trigger class. For symmetric collision systems (Pb–Pb and pp) the data has been symmetrised around $\eta = 0$ and points for $\eta > 3.5$ have been reflected around $\eta = 0$. The boxes around the points and to the right reflect the uncorrelated and correlated, with respect to pseudorapidity, systematic uncertainty, respectively. The relative correlated, normalisation, uncertainties are evaluated at $\mathrm{d}N_{\mathrm{ch}}/\mathrm{d}\eta|_{\eta=0}$. The lines show fits of Eq. (1) (Pb–Pb and pp) and Eq. (2) (p–Pb) to the data (discussed in Section 4). Please note that the ordinate has been cut twice to accommodate for the very different ranges of the charged-particle pseudorapidity densities.

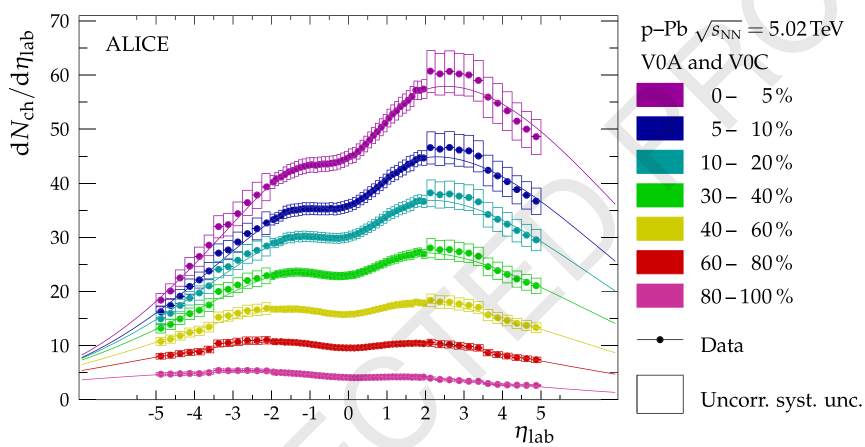

Fig. 2. Charged-particle pseudorapidity density in p–Pb collisions at $\sqrt{s_{\mathrm{NN}}} = 5.02\,\mathrm{TeV}$ in seven centrality classes based on the V0A and V0C estimators. The lines are obtained using a fit of a scaled, normal distribution in rapidity Eq. (2) to the data (discussed in Section 4).

the ratios, systematic uncertainties, of common origin, are partially cancelled, and, as an estimate, the magnitude of the resulting systematic uncertainties are given only by the uncertainties in the $\mathrm{d}N_{\mathrm{ch}}/\mathrm{d}\eta|_X$ measurements, since the uncertainties are independent of the collision system. In p–Pb collisions the rapidity of the centre-of-mass is non-zero, which is not taken into account in the ratios. Such a correction would require prior determination of the full Jacobian of the transformation from pseudorapidity to rapidity, which is not possible to perform reliably with the ALICE apparatus.

The ratio of the p–Pb relative to the pp distributions increases with pseudorapidity from the p-going to the Pb-going direction for central collisions, which Brodsky et al. and Adil et al. [25,26] suggest is a sign of scaling of the pp distribution with the increasing number of participants as the lead nucleus is probed by the incident proton, and thus independent proton–nucleon scatterings on the lead-ion side. A similar scaling, however, does not hold for the Pb–Pb reaction. The ratios cannot be obtained by simple scaling of the elementary pp distributions. Instead, the ratio of the Pb–Pb relative to the pp distributions exhibits an enhancement of particle production around midrapidity for the more central collisions which is indicative of the formation of the sQGP [7]. Likewise, r_{pPb} increases for all but the two most peripheral centrality classes as $\eta_{\mathrm{lab}} \to 3$. In Pb–Pb collisions it is seen that the various mechanisms behind the pseudorapidity distributions are more transversely directed than in pp collisions by the increase of r_{PbPb} as $|\eta| \to 0$

4. Rapidity and energy-density dependence on system size and discussion

It has been shown that the charged-particle *rapidity* density ($\mathrm{d}N_{\mathrm{ch}}/\mathrm{d}y$) in Pb–Pb collisions, to a good accuracy, follows a normal distribution over the considered rapidity interval ($|y| \lesssim 5$) [2,27]. Those results relied on calculating the average Jacobian $\mathrm{d}N_{\mathrm{ch}}/\mathrm{d}y = \langle J\rangle = \langle\beta\rangle$ using the full p_{T} spectra, at midrapidity, of charged pions and kaons as well as protons and antiprotons. Here, we use the approximation

$$y \approx \eta - \frac{1}{2}\frac{m^2}{p_{\mathrm{T}}^2}\cos\vartheta,$$

where ϑ is the polar angle of emission, and identify $a = p_{\mathrm{T}}/m$ with an effective ratio of transverse momentum over mass. With this, the effective Jacobian can be written as

$$J'(\eta, a) = \left(1 + \tfrac{1}{a^2}\tfrac{1}{\cosh^2\eta}\right)^{-1/2}.$$

We further make the ansatz that $\mathrm{d}N_{\mathrm{ch}}/\mathrm{d}y$ is normal distributed for symmetric collision systems (pp and Pb–Pb), so that $\mathrm{d}N_{\mathrm{ch}}/\mathrm{d}\eta$ can be parameterised as

$$f(\eta; A, a, \sigma) = J'(\eta, a)\, A \tfrac{1}{\sqrt{2\pi}\sigma} \exp\left(-\tfrac{y^2\{\eta, a\}}{2\sigma^2}\right), \qquad (1)$$

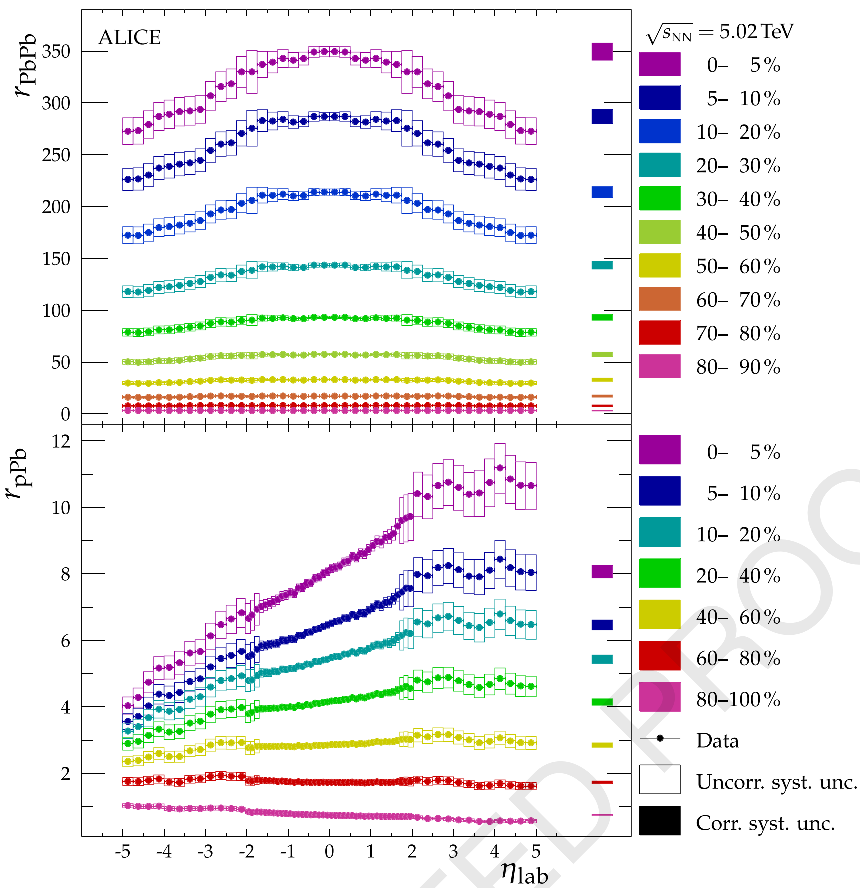

Fig. 3. Ratio r_X of the charged-particle pseudorapidity density in Pb–Pb (top) and p–Pb (bottom) in different centrality classes to the charged-particle pseudorapidity density in pp in the INEL>0 event class. Note, for Pb–Pb $\eta_{\rm lab}$ is the same as the centre-of-mass pseudorapidity.

where A and σ are the total integral and width of the distribution, respectively, and y the rapidity in the centre-of-mass frame. Motivated by the observed approximate linearity of $r_{\rm pPb}$ (see lower panel of Fig. 3), we replace A with $(\alpha y + A)$ for the asymmetric system (p–Pb) and parameterise $\mathrm{d}N_{\rm ch}/\mathrm{d}\eta_{\rm lab}$ as

$$g(\eta; A, a, \alpha, \sigma) = J'(\eta, a)\,(\alpha\, y\{\eta, a\} + A) \times \frac{1}{\sqrt{2\pi}\sigma} \exp\left(-\frac{[y\{\eta,a\} - y_{\rm CM}]^2}{2\sigma^2}\right). \quad (2)$$

The functions f and g defined in Eq. (1) and Eq. (2), respectively, describe the measurements within the measured region with χ^2 per degrees of freedom (ν) in the range of 0.1 to 0.5. The small χ^2/ν values are a consequence of the relatively large uncorrelated systematic uncertainties on the measurements. That is, the charged-particle distributions for pp, p–Pb, and Pb–Pb collisions at $\sqrt{s_{\rm NN}} = 5.02$ TeV follow a normal distribution in rapidity, with free parameters A, a, σ, and α in the asymmetric case.

The top panel of Fig. 4 shows the best-fit parameter values of the normal width ($\sigma_{\mathrm{d}N_{\rm ch}/\mathrm{d}y}$) for all three collision systems as a function of the average number of participating nucleons ($\langle N_{\rm part}\rangle$) calculated using a Glauber model [28]. The best-fit parameters are found taking statistical and uncorrelated systematic uncertainties into account. The result using the above procedure, for the most central Pb–Pb collisions, is found to be compatible with previous results extracted by unfolding with the mean Jacobian estimated from transverse momentum spectra [2]. The open points (crosses) and dashed lines on the figure are from evaluations of Eq. (1) and Eq. (2), and direct calculations of $\sigma_{\mathrm{d}N_{\rm ch}/\mathrm{d}y}$, respectively, using model calculations with EPOS-LHC [29]. EPOS-LHC was chosen as it provides predictions for all three collision systems. The parameterisation, in terms of the two functions, of this model calculation generally reproduces the widths of the charged-particle rapidity densities, except in the asymmetric case where a direct evaluation of the standard deviation is less motivated.

The general trend is that the widths decrease as $\langle N_{\rm part}\rangle$ increases, consistent with the behaviour of the $r_{\rm PbPb}$ ratios. Notably, the width of the $\mathrm{d}N_{\rm ch}/\mathrm{d}y$ distributions in p–Pb and Pb–Pb, for low number of participant nucleons in the collisions, approaches the width of the pp distribution, which, presumably, is dominated by kinematic and phase space constraints.

The lower panel of Fig. 4 shows the dependence of a on the average number of participants. The right-hand ordinate is the same, but multiplied by the average mass $\langle m\rangle = (0.215 \pm 0.001)$ GeV/c^2 estimated from measurements of identified particles in Pb–Pb collisions at $\sqrt{s_{\rm NN}} = 2.76$ TeV [30]. To better understand the parameter a, this parameter extracted from the EPOS-LHC calculations, using the above procedure, is also shown in the figure. The dotted lines show the average $p_{\rm T}/m$ predicted by EPOS-LHC [29]. The EPOS-LHC calculations indicate that the extracted effective transverse momentum to mass ratio a is consistently smaller than the ratio of the average transverse momentum to the average mass. Thus a gives a lower bound on $\langle p_{\rm T}\rangle/\langle m\rangle$.

We can estimate the energy density that is reached in the collisions as a function of the number of participants for the three systems. A conventional approach is to use the model originally proposed by Bjorken [12] in which the energy density ($\varepsilon_{\rm Bj}$) depends on the rapidity density of particles and the volume of a longitudinal cylinder with cross sectional area determined by the overlap between the colliding partners and length determined by a characteristic particle formation time

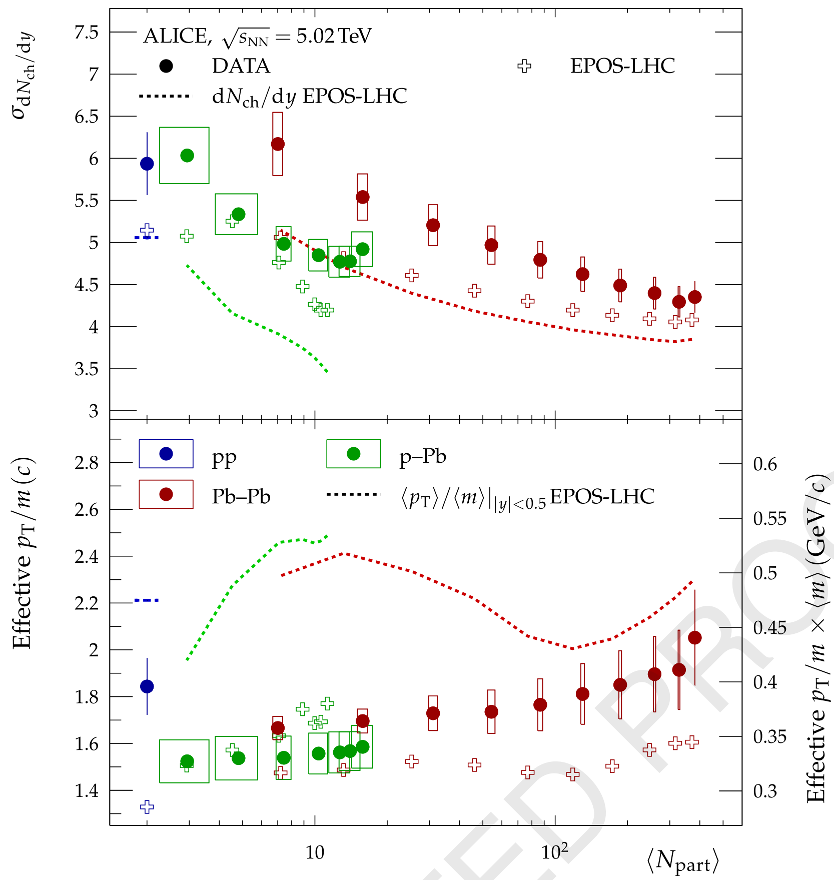

Fig. 4. The width (top) and effective p_T/m (bottom) fit parameters as a function of the mean number of participants in pp, p–Pb, and Pb–Pb collisions at $\sqrt{s_{NN}} = 5.02$ TeV. Vertical uncertainties are the standard error on the best-fit parameter values, while horizontal uncertainties reflect the uncertainty on $\langle N_{part}\rangle$ from the Glauber calculations. Also shown are similar fit parameters from the same parameterisation of EPOS-LHC calculations as well as direct calculations of the standard deviation of the dN_{ch}/dy distributions and the $\langle p_T\rangle/\langle m\rangle$ ratio from the EPOS-LHC calculations.

$$\varepsilon_{Bj} = \frac{1}{c\tau}\frac{1}{S_T}\left\langle\frac{dE_T}{dy}\right\rangle.$$

Here, $S_T \approx \pi R^2 \approx \pi N_{part}^{2/3}$ is the transverse area spanned by the participating nucleons, dE_T/dy is the transverse-energy rapidity density, and τ is the formation time. While a formation time of $\tau = 1$ fm/c is often assumed, it is left as a free parameter here. With $\langle m_T\rangle = \langle m\rangle\sqrt{1+(\langle p_T\rangle/\langle m\rangle)^2}$, the transverse-energy rapidity density can be approximated by

$$\left\langle\frac{dE_T}{dy}\right\rangle \approx \langle m_T\rangle\frac{1}{f_{total}}\frac{dN_{ch}}{dy} = \langle m\rangle\sqrt{1+\left(\frac{\langle p_T\rangle}{\langle m\rangle}\right)^2}\frac{1}{f_{total}}\frac{dN_{ch}}{dy},$$

where $f_{total} = 0.55 \pm 0.01$, the ratio of charged particles to all particles [31], accounts for neutral particles not measured in the experiment, and is assumed the same for all collision systems. Substituting the derived dN_{ch}/dy and the effective $a = p_T/m \lesssim \langle p_T\rangle/\langle m\rangle$ results in a lower bound estimate for the Bjorken energy density (ε_{LB})

$$\varepsilon_{Bj}\tau \geq \varepsilon_{LB}\tau = \frac{1}{c}\frac{1}{S_T}\langle m\rangle\sqrt{1+a^2}\frac{1}{f_{total}}\sqrt{1+\frac{1}{a^2}\frac{1}{\cosh^2\eta}}\frac{dN_{ch}}{d\eta}, \quad (3)$$

where a and $\langle m\rangle$ are as in the top panel of Fig. 4.

The transverse area S_T is estimated in a numerical Glauber model [32,33] as shown in Fig. 5. We consider two extremes for the transverse area spanned by the participating nucleons: a) the *exclusive* (or direct) overlap between participating nucleons, ∩ and open markers in Fig. 5, and b) the *inclusive* (or full) area of all participating nucleons, ∪ and full markers in Fig. 5.

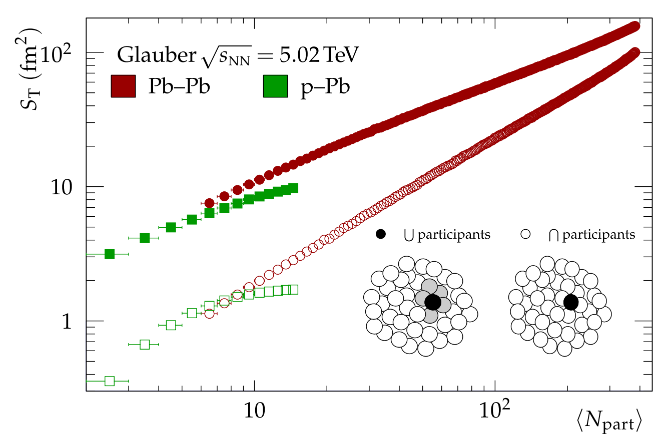

Fig. 5. The transverse area S_T as calculated in a numerical Glauber model for two extreme cases: a) only the exclusive overlap of nucleons is considered (∩, open markers) and b) the inclusive area of participating nucleons contribute (∪, closed markers) in both p–Pb and Pb–Pb at $\sqrt{s_{NN}} = 5.02$ TeV.

Fig. 6 shows the lower-bound energy density estimate, $\varepsilon_{LB}\tau \leq \varepsilon_{Bj}\tau$, as a function of the number of participants, which reaches values between 10 and 20 GeV/(fm^2c) in the most central Pb–Pb collisions. The uncertainties are from standard error propagation of Eq. (3) of uncertainties on the best-fit parameter values, the number of participants, mean mass, and f_{total}. A rise from roughly 1 GeV/(fm^2c) to over 10 GeV/(fm^2c) is observed if the transverse area is assumed to be the inclusive area of participating nucleons. This trend is illustrated by a power-law (CN_{part}^{p}) fit to the data in

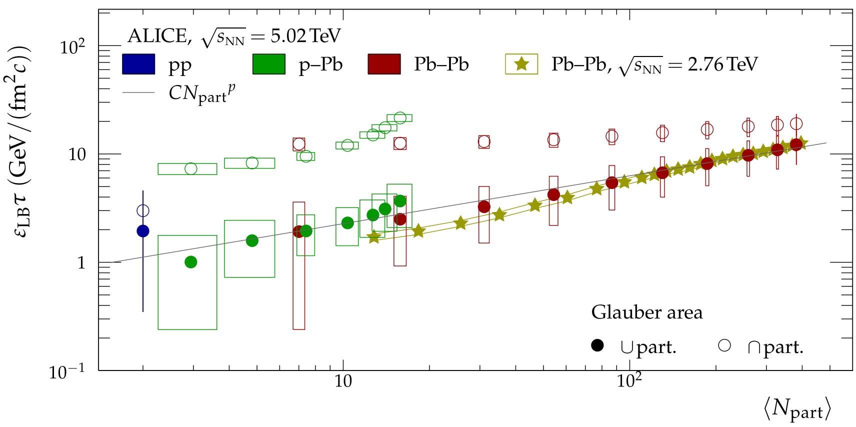

Fig. 6. Estimate of the lower bound on the Bjorken transverse energy density in pp, p–Pb, and Pb–Pb collisions at $\sqrt{s_{\rm NN}} = 5.02$ TeV, considering the exclusive (∩, open markers) and inclusive (∪, full markers) overlap area $S_{\rm T}$ of the nucleons. The expression $CN_{\rm part}{}^{p}$ is fitted to case ∪, and we find $C = (0.8 \pm 0.3)$ GeV/(fm^2c) and $p = 0.44 \pm 0.08$. Also shown is an estimate, via $\mathrm{d}E_{\rm T}/\mathrm{d}y$, of $\varepsilon_{\rm Bj}$ from Pb–Pb collisions at $\sqrt{s_{\rm NN}} = 2.76$ TeV (stars with uncertainty band) [31].

the figure, with the parameter values $C = (0.8 \pm 0.3)$ GeV/(fm^2c) and $p = 0.44 \pm 0.08$. On the other hand, if the transverse area is assumed to be the smaller exclusive overlap area, we observe a substantially larger lower bound on the energy density, but a less dramatic increase with increasing number of participating nucleons. Also shown in the figure are estimates of the Bjorken energy density $\varepsilon_{\rm Bj}\tau$ for Pb–Pb reactions at $\sqrt{s_{\rm NN}} = 2.76$ TeV [31]. These results where obtained from measurements of the transverse energy in the collisions and using the inclusive estimate of the transverse area $S_{\rm T}$. The trend of the $\sqrt{s_{\rm NN}} = 5.02$ TeV results is similar to these earlier results. Bearing in mind that for the largest LHC collision energy we show a lower bound estimate of the energy density in Fig. 6, we find a likely overall increase in the energy density from $\sqrt{s_{\rm NN}} = 2.76$ TeV to 5.02 TeV.

5. Summary and conclusions

We have measured the charged particle pseudorapidity density in pp, p–Pb, and Pb–Pb collisions at $\sqrt{s_{\rm NN}} = 5.02$ TeV over the widest possible pseudorapidity range available at the LHC. The distributions where determined using the same experimental apparatus and methods, and systematic uncertainties have been minimised to within the capabilities of the set-up. While the particle production in central Pb–Pb collisions clearly exhibits an enhancement as compared to pp collisions, particle production in p–Pb collisions is consistent with dominantly incoherent nucleon–nucleon collisions. By transforming the measured pseudorapidity distributions to rapidity distributions we have obtained systematic trends for the width of the rapidity distributions and a lower bound on the energy density, which shows a clear scaling behaviour as a function of the average number of participant nucleons. The decreasing width of the deduced rapidity distributions with increasing participant number suggests that the kinematic spread of particles, including longitudinal degrees of freedom, is reduced due to interactions in the early stages of the collisions. This is also reflected in the accompanying growth of the energy density. Both observations are consistent with the gradual establishment of a high-density phase of matter with increasing size of the collision domain.

Declaration of competing interest

The authors declare that they have no known competing financial interests or personal relationships that could have appeared to influence the work reported in this paper.

Acknowledgements

The ALICE Collaboration would like to thank all its engineers and technicians for their invaluable contributions to the construction of the experiment and the CERN accelerator teams for the outstanding performance of the LHC complex. The ALICE Collaboration gratefully acknowledges the resources and support provided by all Grid centres and the Worldwide LHC Computing Grid (WLCG) collaboration. The ALICE Collaboration acknowledges the following funding agencies for their support in building and running the ALICE detector: A. I. Alikhanyan National Science Laboratory (Yerevan Physics Institute) Foundation (ANSL), State Committee of Science and World Federation of Scientists (WFS), Armenia; Austrian Academy of Sciences, Austrian Science Fund (FWF): [M 2467-N36] and Nationalstiftung für Forschung, Technologie und Entwicklung, Austria; Ministry of Communications and High Technologies, National Nuclear Research Center, Azerbaijan; Conselho Nacional de Desenvolvimento Científico e Tecnológico (CNPq), Financiadora de Estudos e Projetos (Finep), Fundação de Amparo à Pesquisa do Estado de São Paulo (FAPESP) and Universidade Federal do Rio Grande do Sul (UFRGS), Brazil; Ministry of Education of China (MOEC), Ministry of Science & Technology of China (MSTC) and National Natural Science Foundation of China (NSFC), China; Ministry of Science and Education and Croatian Science Foundation, Croatia; Centro de Aplicaciones Tecnológicas y Desarrollo Nuclear (CEADEN), Cubaenergía, Cuba; Ministry of Education, Youth and Sports of the Czech Republic, Czech Republic; The Danish Council for Independent Research | Natural Sciences, the Villum Fonden and Danish National Research Foundation (DNRF), Denmark; Helsinki Institute of Physics (HIP), Finland; Commissariat à l'Energie Atomique (CEA) and Institut National de Physique Nucléaire et de Physique des Particules (IN2P3) and Centre National de la Recherche Scientifique (CNRS), France; Bundesministerium für Bildung und Forschung (BMBF) and GSI Helmholtzzentrum für Schwerionenforschung GmbH, Germany; General Secretariat for Research and Technology, Ministry of Education, Research and Religions, Greece; National Research, Development and Innovation Office, Hungary; Department of Atomic Energy Government of India (DAE), Department of Science and Technology, Government of India (DST), University Grants Commission, Government of India (UGC) and Council of Scientific and Industrial Research (CSIR), India; Indonesian Institute of Sciences, Indonesia; Istituto Nazionale di Fisica Nucleare (INFN), Italy; Japanese Ministry of Education, Culture, Sports, Science and Technology (MEXT) and Japan Society for the Promotion of Science (JSPS) KAKENHI, Japan; Consejo Nacional de Ciencia (CONACYT) y Tecnología, through Fondo de Cooperación Internacional en Ciencia y Tecnología (FONCICYT) and

Dirección General de Asuntos del Personal Académico (DGAPA), Mexico; Nederlandse Organisatie voor Wetenschappelijk Onderzoek (NWO), Netherlands; The Research Council of Norway, Norway; Commission on Science and Technology for Sustainable Development in the South (COMSATS), Pakistan; Pontificia Universidad Católica del Perú, Peru; Ministry of Education and Science, National Science Centre and WUT ID-UB, Poland; Korea Institute of Science and Technology Information and National Research Foundation of Korea (NRF), Republic of Korea; Ministry of Education and Scientific Research, Institute of Atomic Physics, Ministry of Research and Innovation and Institute of Atomic Physics and University Politehnica of Bucharest, Romania; Joint Institute for Nuclear Research (JINR), Ministry of Education and Science of the Russian Federation, National Research Centre Kurchatov Institute, Russian Science Foundation and Russian Foundation for Basic Research, Russia; Ministry of Education, Science, Research and Sport of the Slovak Republic, Slovakia; National Research Foundation of South Africa, South Africa; Swedish Research Council (VR) and Knut and Alice Wallenberg Foundation (KAW), Sweden; European Organization for Nuclear Research, Switzerland; Suranaree University of Technology (SUT), National Science and Technology Development Agency (NSTDA), Thailand Science Research and Innovation (TSRI) and National Science, Research and Innovation Fund (NSRF), Thailand; Turkish Energy, Nuclear and Mineral Research Agency (TENMAK), Turkey; National Academy of Sciences of Ukraine, Ukraine; Science and Technology Facilities Council (STFC), United Kingdom; National Science Foundation of the United States of America (NSF) and United States Department of Energy, Office of Nuclear Physics (DOE NP), United States of America.

References

[1] BRAHMS Collaboration, I.C. Arsene, et al., Nuclear stopping and rapidity loss in Au+Au collisions at $\sqrt{s_{NN}} = 62.4$ GeV, Phys. Lett. B 677 (2009) 267–271, arXiv:0901.0872 [nucl-ex].
[2] ALICE Collaboration, J. Adam, et al., Centrality dependence of the pseudorapidity density distribution for charged particles in Pb–Pb collisions at $\sqrt{s_{NN}} = 5.02$ TeV, Phys. Lett. B 772 (2017) 567–577, arXiv:1612.08966 [nucl-ex].
[3] NA50 Collaboration, M.C. Abreu, et al., Scaling of charged particle multiplicity in Pb-Pb collisions at SPS energies, Phys. Lett. B 530 (2002) 43–55.
[4] PHOBOS Collaboration, B. Alver, et al., Charged-particle multiplicity and pseudorapidity distributions measured with the PHOBOS detector in Au+Au, Cu+Cu, d+Au, p+p collisions at ultrarelativistic energies, Phys. Rev. C 83 (2011) 024913, arXiv:1011.1940 [nucl-ex].
[5] ATLAS Collaboration, G. Aad, et al., Measurement of the centrality dependence of the charged-particle pseudorapidity distribution in proton–lead collisions at $\sqrt{s_{NN}} = 5.02$ TeV with the ATLAS detector, Eur. Phys. J. C 76 (2016) 199, arXiv:1508.00848 [hep-ex].
[6] BRAHMS Collaboration, I. Arsene, et al., Quark gluon plasma and color glass condensate at RHIC? The perspective from the BRAHMS experiment, Nucl. Phys. A 757 (2005) 1–27, arXiv:nucl-ex/0410020 [nucl-ex].
[7] PHOBOS Collaboration, B.B. Back, et al., The PHOBOS perspective on discoveries at RHIC, Nucl. Phys. A 757 (2005) 28–101, arXiv:nucl-ex/0410022 [nucl-ex].
[8] STAR Collaboration, J. Adams, et al., Experimental and theoretical challenges in the search for the quark gluon plasma: the STAR Collaboration's critical assessment of the evidence from RHIC collisions, Nucl. Phys. A 757 (2005) 102–183, arXiv:nucl-ex/0501009 [nucl-ex].
[9] PHENIX Collaboration, K. Adcox, et al., Formation of dense partonic matter in relativistic nucleus-nucleus collisions at RHIC: experimental evaluation by the PHENIX collaboration, Nucl. Phys. A 757 (2005) 184–283, arXiv:nucl-ex/0410003 [nucl-ex].
[10] C. Bierlich, T. Sjöstrand, M. Utheim, Hadronic rescattering in pA and AA collisions, Eur. Phys. J. A 57 (2021) 227, arXiv:2103.09665 [hep-ph].
[11] Z.-W. Lin, L. Zheng, Further developments of a multi-phase transport model for relativistic nuclear collisions, Nucl. Sci. Tech. 32 (2021) 113, arXiv:2110.02989 [nucl-th].
[12] J.D. Bjorken, Highly relativistic nucleus-nucleus collisions: the central rapidity region, Phys. Rev. D 27 (Jan 1983) 140–151.
[13] H.-T. Ding, Recent lattice QCD results and phase diagram of strongly interacting matter, Nucl. Phys. A 931 (2014) 52–62, arXiv:1408.5236 [hep-lat].
[14] ALICE Collaboration, K. Aamodt, et al., The ALICE experiment at the CERN LHC, J. Instrum. 3 (2008) S08002.
[15] ALICE Collaboration, B. Abelev, et al., Performance of the ALICE experiment at the CERN LHC, Int. J. Mod. Phys. A 29 (2014) 1430044, arXiv:1402.4476 [nucl-ex].
[16] ALICE Collaboration, J. Adam, et al., Charged-particle multiplicities in proton–proton collisions at $\sqrt{s} = 0.9$ to 8 TeV, Eur. Phys. J. C 77 (2017) 33, arXiv:1509.07541 [nucl-ex].
[17] ALICE Collaboration, S. Acharya, et al., Pseudorapidity distributions of charged particles as a function of mid- and forward rapidity multiplicities in pp collisions at $\sqrt{s} = 5.02$, 7 and 13 TeV, Eur. Phys. J. C 81 (2021) 630, arXiv:2009.09434 [nucl-ex].
[18] ALICE Collaboration, K. Aamodt, et al., Charged–particle multiplicity density at mid–rapidity in central Pb–Pb collisions at $\sqrt{s_{NN}} = 2.76$ TeV, Phys. Rev. Lett. 105 (2010) 252301, arXiv:1011.3916 [nucl-ex].
[19] ALICE Collaboration, B. Abelev, et al., Centrality determination of Pb-Pb collisions at $\sqrt{s_{NN}} = 2.76$ TeV with ALICE, Phys. Rev. C 88 (2013) 044909, arXiv:1301.4361 [nucl-ex].
[20] ALICE Collaboration, J. Adam, et al., Centrality dependence of particle production in p-Pb collisions at $\sqrt{s_{NN}} = 5.02$ TeV, Phys. Rev. C 91 (2015) 064905, arXiv:1412.6828 [nucl-ex].
[21] ALICE Collaboration, S. Acharya, et al., The ALICE definition of primary particles, ALICE-PUBLIC-2017-005, https://cds.cern.ch/record/2270008.
[22] ALICE Collaboration, J. Adam, et al., Centrality evolution of the charged-particle pseudorapidity density over a broad pseudorapidity range in Pb-Pb collisions at $\sqrt{s_{NN}} = 2.76$ TeV, Phys. Lett. B 754 (2016) 373–385, arXiv:1509.07299 [nucl-ex].
[23] ALICE Collaboration, J. Adam, et al., Centrality dependence of the charged-particle multiplicity density at midrapidity in Pb-Pb collisions at $\sqrt{s_{NN}} = 5.02$ TeV, Phys. Rev. Lett. 116 (2016) 222302, arXiv:1512.06104 [nucl-ex].
[24] ALICE Collaboration, S. Acharya, et al., Charged-particle production as a function of multiplicity and transverse spherocity in pp collisions at $\sqrt{s} = 5.02$ and 13 TeV, Eur. Phys. J. C 79 (2019) 857, arXiv:1905.07208 [nucl-ex].
[25] S.J. Brodsky, et al., Hadron production in nuclear collisions: a new parton model approach, Phys. Rev. Lett. 39 (1977) 1120.
[26] A. Adil, et al., 3D jet tomography of twisted strongly coupled quark gluon plasmas, Phys. Rev. C 72 (2005) 034907, arXiv:nucl-th/0505004 [nucl-th].
[27] ALICE Collaboration, E. Abbas, et al., Centrality dependence of the pseudorapidity density distribution for charged particles in Pb–Pb collisions at $\sqrt{s_{NN}} = 2.76$ TeV, Phys. Lett. B 726 (2013) 610–622, arXiv:1304.0347 [nucl-ex].
[28] ALICE Collaboration, S. Acharya, et al., Centrality determination in heavy ion collisions, ALICE-PUBLIC-2018-011, http://cds.cern.ch/record/2636623.
[29] T. Pierog, et al., EPOS LHC: test of collective hadronization with data measured at the CERN Large Hadron Collider, Phys. Rev. C 92 (2015) 034906, arXiv:1306.0121 [hep-ph].
[30] ALICE Collaboration, B. Abelev, et al., Centrality dependence of π, K, p production in Pb-Pb collisions at $\sqrt{s_{NN}} = 2.76$ TeV, Phys. Rev. C 88 (2013) 044910, arXiv:1303.0737 [hep-ex].
[31] ALICE Collaboration, J. Adam, et al., Measurement of transverse energy at midrapidity in Pb–Pb collisions at $\sqrt{s_{NN}} = 2.76$ TeV, Phys. Rev. C 94 (2016) 034903, arXiv:1603.04775 [nucl-ex].
[32] C. Loizides, J. Nagle, P. Steinberg, Improved version of the PHOBOS Glauber Monte Carlo, SoftwareX 1–2 (2015) 13–18.
[33] C. Loizides, Glauber modeling of high-energy nuclear collisions at the subnucleon level, Phys. Rev. C 94 (2016) 024914, arXiv:1603.07375 [nucl-ex].

ALICE Collaboration

S. Acharya [142], D. Adamová [96], A. Adler [74], J. Adolfsson [81], G. Aglieri Rinella [34], M. Agnello [30], N. Agrawal [54], Z. Ahammed [142], S. Ahmad [16], S.U. Ahn [76], I. Ahuja [38], Z. Akbar [51], A. Akindinov [93], M. Al-Turany [108], S.N. Alam [16], D. Aleksandrov [89], B. Alessandro [59], H.M. Alfanda [7], R. Alfaro Molina [71], B. Ali [16], Y. Ali [14], A. Alici [25], N. Alizadehvandchali [125], A. Alkin [34], J. Alme [21], G. Alocco [55], T. Alt [68], I. Altsybeev [113], M.N. Anaam [7], C. Andrei [48], A. Andronic [145], V. Anguelov [105], F. Antinori [57], P. Antonioli [54], C. Anuj [16], N. Apadula [80], L. Aphecetche [115], H. Appelshäuser [68], S. Arcelli [25], R. Arnaldi [59], I.C. Arsene [20],

M. Arslandok[147], A. Augustinus[34], R. Averbeck[108], S. Aziz[78], M.D. Azmi[16], A. Badalà[56], Y.W. Baek[41], X. Bai[129,108], R. Bailhache[68], Y. Bailung[50], R. Bala[102], A. Balbino[30], A. Baldisseri[139], B. Balis[2], D. Banerjee[4], Z. Banoo[102], R. Barbera[26], L. Barioglio[106], M. Barlou[85], G.G. Barnaföldi[146], L.S. Barnby[95], V. Barret[136], C. Bartels[128], K. Barth[34], E. Bartsch[68], F. Baruffaldi[27], N. Bastid[136], S. Basu[81], G. Batigne[115], D. Battistini[106], B. Batyunya[75], D. Bauri[49], J.L. Bazo Alba[112], I.G. Bearden[90], C. Beattie[147], P. Becht[108], I. Belikov[138], A.D.C. Bell Hechavarria[145], F. Bellini[25], R. Bellwied[125], S. Belokurova[113], V. Belyaev[94], G. Bencedi[146,69], S. Beole[24], A. Bercuci[48], Y. Berdnikov[99], A. Berdnikova[105], L. Bergmann[105], M.G. Besoiu[67], L. Betev[34], P.P. Bhaduri[142], A. Bhasin[102], I.R. Bhat[102], M.A. Bhat[4], B. Bhattacharjee[42], L. Bianchi[24], N. Bianchi[52], J. Bielčík[37], J. Bielčíková[96], J. Biernat[118], A. Bilandzic[106], G. Biro[146], S. Biswas[4], J.T. Blair[119], D. Blau[89,82], M.B. Blidaru[108], C. Blume[68], G. Boca[28,58], F. Bock[97], A. Bogdanov[94], S. Boi[22], J. Bok[61], L. Boldizsár[146], A. Bolozdynya[94], M. Bombara[38], P.M. Bond[34], G. Bonomi[141,58], H. Borel[139], A. Borissov[82], H. Bossi[147], E. Botta[24], L. Bratrud[68], P. Braun-Munzinger[108], M. Bregant[121], M. Broz[37], G.E. Bruno[107,33], M.D. Buckland[23,128], D. Budnikov[109], H. Buesching[68], S. Bufalino[30], O. Bugnon[115], P. Buhler[114], Z. Buthelezi[72,132], J.B. Butt[14], A. Bylinkin[21,127], S.A. Bysiak[118], M. Cai[27,7], H. Caines[147], A. Caliva[108], E. Calvo Villar[112], J.M.M. Camacho[120], R.S. Camacho[45], P. Camerini[23], F.D.M. Canedo[121], M. Carabas[135], F. Carnesecchi[34,25], R. Caron[137,139], J. Castillo Castellanos[139], F. Catalano[30], C. Ceballos Sanchez[75], I. Chakaberia[80], P. Chakraborty[49], S. Chandra[142], S. Chapeland[34], M. Chartier[128], S. Chattopadhyay[142], S. Chattopadhyay[110], T.G. Chavez[45], T. Cheng[7], C. Cheshkov[137], B. Cheynis[137], V. Chibante Barroso[34], D.D. Chinellato[122], E.S. Chizzali[106], S. Cho[61], P. Chochula[34], P. Christakoglou[91], C.H. Christensen[90], P. Christiansen[81], T. Chujo[134], C. Cicalo[55], L. Cifarelli[25], F. Cindolo[54], M.R. Ciupek[108], G. Clai[54,II], J. Cleymans[124,I], F. Colamaria[53], J.S. Colburn[111], D. Colella[53,107,33], A. Collu[80], M. Colocci[25,34], M. Concas[59,III], G. Conesa Balbastre[79], Z. Conesa del Valle[78], G. Contin[23], J.G. Contreras[37], M.L. Coquet[139], T.M. Cormier[97], P. Cortese[31], M.R. Cosentino[123], F. Costa[34], S. Costanza[28,58], P. Crochet[136], R. Cruz-Torres[80], E. Cuautle[69], P. Cui[7], L. Cunqueiro[97], A. Dainese[57], M.C. Danisch[105], A. Danu[67], P. Das[87], P. Das[4], S. Das[4], S. Dash[49], A. De Caro[29], G. de Cataldo[53], L. De Cilladi[24], J. de Cuveland[39], A. De Falco[22], D. De Gruttola[29], N. De Marco[59], C. De Martin[23], S. De Pasquale[29], S. Deb[50], H.F. Degenhardt[121], K.R. Deja[143], R. Del Grande[106], L. Dello Stritto[29], W. Deng[7], P. Dhankher[19], D. Di Bari[33], A. Di Mauro[34], R.A. Diaz[75,8], T. Dietel[124], Y. Ding[137,7], R. Divià[34], D.U. Dixit[19], Ø. Djuvsland[21], U. Dmitrieva[63], A. Dobrin[67], B. Dönigus[68], A.K. Dubey[142], A. Dubla[108,91], S. Dudi[101], P. Dupieux[136], M. Durkac[117], N. Dzalaiova[13], T.M. Eder[145], R.J. Ehlers[97], V.N. Eikeland[21], F. Eisenhut[68], D. Elia[53], B. Erazmus[115], F. Ercolessi[25], E. Eremenko[96], F. Erhardt[100], A. Erokhin[113], M.R. Ersdal[21], B. Espagnon[78], G. Eulisse[34], D. Evans[111], S. Evdokimov[92], L. Fabbietti[106], M. Faggin[27], J. Faivre[79], F. Fan[7], W. Fan[80], A. Fantoni[52], M. Fasel[97], P. Fecchio[30], A. Feliciello[59], G. Feofilov[113], A. Fernández Téllez[45], A. Ferrero[139], A. Ferretti[24], V.J.G. Feuillard[105], J. Figiel[118], V. Filova[37], D. Finogeev[63], F.M. Fionda[55], G. Fiorenza[34], F. Flor[125], A.N. Flores[119], S. Foertsch[72], S. Fokin[89], E. Fragiacomo[60], E. Frajna[146], A. Francisco[136], U. Fuchs[34], N. Funicello[29], C. Furget[79], A. Furs[63], J.J. Gaardhøje[90], M. Gagliardi[24], A.M. Gago[112], A. Gal[138], C.D. Galvan[120], P. Ganoti[85], C. Garabatos[108], J.R.A. Garcia[45], E. Garcia-Solis[10], K. Garg[115], C. Gargiulo[34], A. Garibli[88], K. Garner[145], P. Gasik[108], E.F. Gauger[119], A. Gautam[127], M.B. Gay Ducati[70], M. Germain[115], S.K. Ghosh[4], M. Giacalone[25], P. Gianotti[52], P. Giubellino[108,59], P. Giubilato[27], A.M.C. Glaenzer[139], P. Glässel[105], E. Glimos[131], D.J.Q. Goh[83], V. Gonzalez[144], L.H. González-Trueba[71], S. Gorbunov[39], M. Gorgon[2], L. Görlich[118], S. Gotovac[35], V. Grabski[71], L.K. Graczykowski[143], L. Greiner[80], A. Grelli[62], C. Grigoras[34], V. Grigoriev[94], S. Grigoryan[75,1], F. Grosa[34,59], J.F. Grosse-Oetringhaus[34], R. Grosso[108], D. Grund[37], G.G. Guardiano[122], R. Guernane[79], M. Guilbaud[115], K. Gulbrandsen[90], T. Gunji[133], W. Guo[7], A. Gupta[102], R. Gupta[102], S.P. Guzman[45], L. Gyulai[146], M.K. Habib[108], C. Hadjidakis[78], H. Hamagaki[83], M. Hamid[7], R. Hannigan[119], M.R. Haque[143], A. Harlenderova[108], J.W. Harris[147], A. Harton[10], J.A. Hasenbichler[34], H. Hassan[97], D. Hatzifotiadou[54], P. Hauer[43], L.B. Havener[147], S.T. Heckel[106], E. Hellbär[108], H. Helstrup[36], T. Herman[37], G. Herrera Corral[9], F. Herrmann[145], K.F. Hetland[36], B. Heybeck[68], H. Hillemanns[34], C. Hills[128], B. Hippolyte[138], B. Hofman[62], B. Hohlweger[91], J. Honermann[145], G.H. Hong[148], D. Horak[37], S. Hornung[108], A. Horzyk[2], R. Hosokawa[15], Y. Hou[7], P. Hristov[34], C. Hughes[131], P. Huhn[68], L.M. Huhta[126], C.V. Hulse[78], T.J. Humanic[98], H. Hushnud[110], L.A. Husova[145], A. Hutson[125], J.P. Iddon[128], R. Ilkaev[109], H. Ilyas[14], M. Inaba[134], G.M. Innocenti[34], M. Ippolitov[89], A. Isakov[96], T. Isidori[127], M.S. Islam[110], M. Ivanov[108], V. Ivanov[99], V. Izucheev[92],

M. Jablonski[2], B. Jacak[80], N. Jacazio[34], P.M. Jacobs[80], S. Jadlovska[117], J. Jadlovsky[117], S. Jaelani[62], C. Jahnke[122], M.J. Jakubowska[143], A. Jalotra[102], M.A. Janik[143], T. Janson[74], M. Jercic[100], O. Jevons[111], A.A.P. Jimenez[69], F. Jonas[97,145], P.G. Jones[111], J.M. Jowett[34,108], J. Jung[68], M. Jung[68], A. Junique[34], A. Jusko[111], M.J. Kabus[143], J. Kaewjai[116], P. Kalinak[64], A.S. Kalteyer[108], A. Kalweit[34], V. Kaplin[94], A. Karasu Uysal[77], D. Karatovic[100], O. Karavichev[63], T. Karavicheva[63], P. Karczmarczyk[143], E. Karpechev[63], V. Kashyap[87], A. Kazantsev[89], U. Kebschull[74], R. Keidel[47], D.L.D. Keijdener[62], M. Keil[34], B. Ketzer[43], A.M. Khan[7], S. Khan[16], A. Khanzadeev[99], Y. Kharlov[92,82], A. Khatun[16], A. Khuntia[118], B. Kileng[36], B. Kim[17], C. Kim[17], D.J. Kim[126], E.J. Kim[73], J. Kim[148], J.S. Kim[41], J. Kim[105], J. Kim[73], M. Kim[105], S. Kim[18], T. Kim[148], S. Kirsch[68], I. Kisel[39], S. Kiselev[93], A. Kisiel[143], J.P. Kitowski[2], J.L. Klay[6], J. Klein[34], S. Klein[80], C. Klein-Bösing[145], M. Kleiner[68], T. Klemenz[106], A. Kluge[34], A.G. Knospe[125], C. Kobdaj[116], T. Kollegger[108], A. Kondratyev[75], N. Kondratyeva[94], E. Kondratyuk[92], J. Konig[68], S.A. Konigstorfer[106], P.J. Konopka[34], G. Kornakov[143], S.D. Koryciak[2], A. Kotliarov[96], O. Kovalenko[86], V. Kovalenko[113], M. Kowalski[118], I. Králik[64], A. Kravčáková[38], L. Kreis[108], M. Krivda[111,64], F. Krizek[96], K. Krizkova Gajdosova[37], M. Kroesen[105], M. Krüger[68], D.M. Krupova[37], E. Kryshen[99], M. Krzewicki[39], V. Kučera[34], C. Kuhn[138], P.G. Kuijer[91], T. Kumaoka[134], D. Kumar[142], L. Kumar[101], N. Kumar[101], S. Kundu[34], P. Kurashvili[86], A. Kurepin[63], A.B. Kurepin[63], A. Kuryakin[109], S. Kushpil[96], J. Kvapil[111], M.J. Kweon[61], J.Y. Kwon[61], Y. Kwon[148], S.L. La Pointe[39], P. La Rocca[26], Y.S. Lai[80], A. Lakrathok[116], M. Lamanna[34], R. Langoy[130], P. Larionov[34,52], E. Laudi[34], L. Lautner[34,106], R. Lavicka[114,37], T. Lazareva[113], R. Lea[141,58], J. Lehrbach[39], R.C. Lemmon[95], I. León Monzón[120], M.M. Lesch[106], E.D. Lesser[19], M. Lettrich[34,106], P. Lévai[146], X. Li[11], X.L. Li[7], J. Lien[130], R. Lietava[111], B. Lim[17], S.H. Lim[17], V. Lindenstruth[39], A. Lindner[48], C. Lippmann[108], A. Liu[19], D.H. Liu[7], J. Liu[128], I.M. Lofnes[21], V. Loginov[94], C. Loizides[97], P. Loncar[35], J.A. Lopez[105], X. Lopez[136], E. López Torres[8], J.R. Luhder[145], M. Lunardon[27], G. Luparello[60], Y.G. Ma[40], A. Maevskaya[63], M. Mager[34], T. Mahmoud[43], A. Maire[138], M. Malaev[99], N.M. Malik[102], Q.W. Malik[20], S.K. Malik[102], L. Malinina[75,IV], D. Mal'Kevich[93], D. Mallick[87], N. Mallick[50], G. Mandaglio[32,56], V. Manko[89], F. Manso[136], V. Manzari[53], Y. Mao[7], G.V. Margagliotti[23], A. Margotti[54], A. Marín[108], C. Markert[119], M. Marquard[68], N.A. Martin[105], P. Martinengo[34], J.L. Martinez[125], M.I. Martínez[45], G. Martínez García[115], S. Masciocchi[108], M. Masera[24], A. Masoni[55], L. Massacrier[78], A. Mastroserio[140,53], A.M. Mathis[106], O. Matonoha[81], P.F.T. Matuoka[121], A. Matyja[118], C. Mayer[118], A.L. Mazuecos[34], F. Mazzaschi[24], M. Mazzilli[34], J.E. Mdhluli[132], A.F. Mechler[68], Y. Melikyan[63], A. Menchaca-Rocha[71], E. Meninno[114,29], A.S. Menon[125], M. Meres[13], S. Mhlanga[124,72], Y. Miake[134], L. Micheletti[59], L.C. Migliorin[137], D.L. Mihaylov[106], K. Mikhaylov[75,93], A.N. Mishra[146], D. Miśkowiec[108], A. Modak[4], A.P. Mohanty[62], B. Mohanty[87], M. Mohisin Khan[16,V], M.A. Molander[44], Z. Moravcova[90], C. Mordasini[106], D.A. Moreira De Godoy[145], I. Morozov[63], A. Morsch[34], T. Mrnjavac[34], V. Muccifora[52], E. Mudnic[35], S. Muhuri[142], J.D. Mulligan[80], A. Mulliri[22], M.G. Munhoz[121], R.H. Munzer[68], H. Murakami[133], S. Murray[124], L. Musa[34], J. Musinsky[64], J.W. Myrcha[143], B. Naik[132], R. Nair[86], B.K. Nandi[49], R. Nania[54], E. Nappi[53], A.F. Nassirpour[81], A. Nath[105], C. Nattrass[131], A. Neagu[20], A. Negru[135], L. Nellen[69], S.V. Nesbo[36], G. Neskovic[39], D. Nesterov[113], B.S. Nielsen[90], E.G. Nielsen[90], S. Nikolaev[89], S. Nikulin[89], V. Nikulin[99], F. Noferini[54], S. Noh[12], P. Nomokonov[75], J. Norman[128], N. Novitzky[134], P. Nowakowski[143], A. Nyanin[89], J. Nystrand[21], M. Ogino[83], A. Ohlson[81], V.A. Okorokov[94], J. Oleniacz[143], A.C. Oliveira Da Silva[131], M.H. Oliver[147], A. Onnerstad[126], C. Oppedisano[59], A. Ortiz Velasquez[69], T. Osako[46], A. Oskarsson[81], J. Otwinowski[118], M. Oya[46], K. Oyama[83], Y. Pachmayer[105], S. Padhan[49], D. Pagano[141,58], G. Paić[69], A. Palasciano[53], S. Panebianco[139], J. Park[61], J.E. Parkkila[126], S.P. Pathak[125], R.N. Patra[102,34], B. Paul[22], H. Pei[7], T. Peitzmann[62], X. Peng[7], L.G. Pereira[70], H. Pereira Da Costa[139], D. Peresunko[89,82], G.M. Perez[8], S. Perrin[139], Y. Pestov[5], V. Petráček[37], V. Petrov[113], M. Petrovici[48], R.P. Pezzi[115,70], S. Piano[60], M. Pikna[13], P. Pillot[115], O. Pinazza[54,34], L. Pinsky[125], C. Pinto[26], S. Pisano[52], M. Płoskoń[80], M. Planinic[100], F. Pliquett[68], M.G. Poghosyan[97], B. Polichtchouk[92], S. Politano[30], N. Poljak[100], A. Pop[48], S. Porteboeuf-Houssais[136], J. Porter[80], V. Pozdniakov[75], S.K. Prasad[4], R. Preghenella[54], F. Prino[59], C.A. Pruneau[144], I. Pshenichnov[63], M. Puccio[34], S. Qiu[91], L. Quaglia[24], R.E. Quishpe[125], S. Ragoni[111], A. Rakotozafindrabe[139], L. Ramello[31], F. Rami[138], S.A.R. Ramirez[45], T.A. Rancien[79], R. Raniwala[103], S. Raniwala[103], S.S. Räsänen[44], R. Rath[50], I. Ravasenga[91], K.F. Read[97,131], A.R. Redelbach[39], K. Redlich[86,VI], A. Rehman[21], P. Reichelt[68], F. Reidt[34], H.A. Reme-ness[36], Z. Rescakova[38], K. Reygers[105], A. Riabov[99], V. Riabov[99], T. Richert[81], M. Richter[20], W. Riegler[34], F. Riggi[26], C. Ristea[67],

M. Rodríguez Cahuantzi[45], K. Røed[20], R. Rogalev[92], E. Rogochaya[75], T.S. Rogoschinski[68], D. Rohr[34], D. Röhrich[21], P.F. Rojas[45], S. Rojas Torres[37], P.S. Rokita[143], F. Ronchetti[52], A. Rosano[32,56], E.D. Rosas[69], A. Rossi[57], A. Roy[50], P. Roy[110], S. Roy[49], N. Rubini[25], O.V. Rueda[81], D. Ruggiano[143], R. Rui[23], B. Rumyantsev[75], P.G. Russek[2], R. Russo[91], A. Rustamov[88], E. Ryabinkin[89], Y. Ryabov[99], A. Rybicki[118], H. Rytkonen[126], W. Rzesa[143], O.A.M. Saarimaki[44], R. Sadek[115], S. Sadovsky[92], J. Saetre[21], K. Šafařík[37], S.K. Saha[142], S. Saha[87], B. Sahoo[49], P. Sahoo[49], R. Sahoo[50], S. Sahoo[65], D. Sahu[50], P.K. Sahu[65], J. Saini[142], S. Sakai[134], M.P. Salvan[108], S. Sambyal[102], T.B. Saramela[121], D. Sarkar[144], N. Sarkar[142], P. Sarma[42], V.M. Sarti[106], M.H.P. Sas[147], J. Schambach[97], H.S. Scheid[68], C. Schiaua[48], R. Schicker[105], A. Schmah[105], C. Schmidt[108], H.R. Schmidt[104], M.O. Schmidt[34,105], M. Schmidt[104], N.V. Schmidt[97,68], A.R. Schmier[131], R. Schotter[138], J. Schukraft[34], K. Schwarz[108], K. Schweda[108], G. Scioli[25], E. Scomparin[59], J.E. Seger[15], Y. Sekiguchi[133], D. Sekihata[133], I. Selyuzhenkov[108,94], S. Senyukov[138], J.J. Seo[61], D. Serebryakov[63], L. Šerkšnytė[106], A. Sevcenco[67], T.J. Shaba[72], A. Shabanov[63], A. Shabetai[115], R. Shahoyan[34], W. Shaikh[110], A. Shangaraev[92], A. Sharma[101], D. Sharma[49], H. Sharma[118], M. Sharma[102], N. Sharma[101], S. Sharma[102], U. Sharma[102], A. Shatat[78], O. Sheibani[125], K. Shigaki[46], M. Shimomura[84], S. Shirinkin[93], Q. Shou[40], Y. Sibiriak[89], S. Siddhanta[55], T. Siemiarczuk[86], T.F. Silva[121], D. Silvermyr[81], T. Simantathammakul[116], G. Simonetti[34], B. Singh[106], R. Singh[87], R. Singh[102], R. Singh[50], V.K. Singh[142], V. Singhal[142], T. Sinha[110], B. Sitar[13], M. Sitta[31], T.B. Skaali[20], G. Skorodumovs[105], M. Slupecki[44], N. Smirnov[147], R.J.M. Snellings[62], C. Soncco[112], J. Song[125], A. Songmoolnak[116], F. Soramel[27], S. Sorensen[131], I. Sputowska[118], J. Stachel[105], I. Stan[67], P.J. Steffanic[131], S.F. Stiefelmaier[105], D. Stocco[115], I. Storehaug[20], M.M. Storetvedt[36], P. Stratmann[145], S. Strazzi[25], C.P. Stylianidis[91], A.A.P. Suaide[121], C. Suire[78], M. Sukhanov[63], M. Suljic[34], R. Sultanov[93], V. Sumberia[102], S. Sumowidagdo[51], S. Swain[65], A. Szabo[13], I. Szarka[13], U. Tabassam[14], S.F. Taghavi[106], G. Taillepied[108,136], J. Takahashi[122], G.J. Tambave[21], S. Tang[136,7], Z. Tang[129], J.D. Tapia Takaki[127,VII], N. Tapus[135], M.G. Tarzila[48], A. Tauro[34], G. Tejeda Muñoz[45], A. Telesca[34], L. Terlizzi[24], C. Terrevoli[125], G. Tersimonov[3], S. Thakur[142], D. Thomas[119], R. Tieulent[137], A. Tikhonov[63], A.R. Timmins[125], M. Tkacik[117], A. Toia[68], N. Topilskaya[63], M. Toppi[52], F. Torales-Acosta[19], T. Tork[78], A.G. Torres Ramos[33], A. Trifiró[32,56], A.S. Triolo[32], S. Tripathy[54], T. Tripathy[49], S. Trogolo[34], V. Trubnikov[3], W.H. Trzaska[126], T.P. Trzcinski[143], A. Tumkin[109], R. Turrisi[57], T.S. Tveter[20], K. Ullaland[21], A. Uras[137], M. Urioni[58,141], G.L. Usai[22], M. Vala[38], N. Valle[28], S. Vallero[59], L.V.R. van Doremalen[62], M. van Leeuwen[91], P. Vande Vyvre[34], D. Varga[146], Z. Varga[146], M. Varga-Kofarago[146], M. Vasileiou[85], A. Vasiliev[89], O. Vázquez Doce[52,106], V. Vechernin[113], A. Velure[21], E. Vercellin[24], S. Vergara Limón[45], L. Vermunt[62], R. Vértesi[146], M. Verweij[62], L. Vickovic[35], Z. Vilakazi[132], O. Villalobos Baillie[111], G. Vino[53], A. Vinogradov[89], T. Virgili[29], V. Vislavicius[90], A. Vodopyanov[75], B. Volkel[34], M.A. Völkl[105], K. Voloshin[93], S.A. Voloshin[144], G. Volpe[33], B. von Haller[34], I. Vorobyev[106], N. Vozniuk[63], J. Vrláková[38], B. Wagner[21], C. Wang[40], D. Wang[40], M. Weber[114], R.J.G.V. Weelden[91], A. Wegrzynek[34], S.C. Wenzel[34], J.P. Wessels[145], S.L. Weyhmiller[147], J. Wiechula[68], J. Wikne[20], G. Wilk[86], J. Wilkinson[108], G.A. Willems[145], B. Windelband[105], M. Winn[139], W.E. Witt[131], J.R. Wright[119], W. Wu[40], Y. Wu[129], R. Xu[7], A.K. Yadav[142], S. Yalcin[77], Y. Yamaguchi[46], K. Yamakawa[46], S. Yang[21], S. Yano[46], Z. Yin[7], I.-K. Yoo[17], J.H. Yoon[61], S. Yuan[21], A. Yuncu[105], V. Zaccolo[23], C. Zampolli[34], H.J.C. Zanoli[62], F. Zanone[105], N. Zardoshti[34,111], A. Zarochentsev[113], P. Závada[66], N. Zaviyalov[109], M. Zhalov[99], B. Zhang[7], S. Zhang[40], X. Zhang[7], Y. Zhang[129], V. Zherebchevskii[113], Y. Zhi[11], N. Zhigareva[93], D. Zhou[7], Y. Zhou[90], J. Zhu[108,7], Y. Zhu[7], G. Zinovjev[3,I], N. Zurlo[141,58]

[1] *A.I. Alikhanyan National Science Laboratory (Yerevan Physics Institute) Foundation, Yerevan, Armenia*
[2] *AGH University of Science and Technology, Cracow, Poland*
[3] *Bogolyubov Institute for Theoretical Physics, National Academy of Sciences of Ukraine, Kiev, Ukraine*
[4] *Bose Institute, Department of Physics and Centre for Astroparticle Physics and Space Science (CAPSS), Kolkata, India*
[5] *Budker Institute for Nuclear Physics, Novosibirsk, Russia*
[6] *California Polytechnic State University, San Luis Obispo, CA, United States*
[7] *Central China Normal University, Wuhan, China*
[8] *Centro de Aplicaciones Tecnológicas y Desarrollo Nuclear (CEADEN), Havana, Cuba*
[9] *Centro de Investigación y de Estudios Avanzados (CINVESTAV), Mexico City and Mérida, Mexico*
[10] *Chicago State University, Chicago, IL, United States*
[11] *China Institute of Atomic Energy, Beijing, China*
[12] *Chungbuk National University, Cheongju, Republic of Korea*
[13] *Comenius University Bratislava, Faculty of Mathematics, Physics and Informatics, Bratislava, Slovakia*
[14] *COMSATS University Islamabad, Islamabad, Pakistan*
[15] *Creighton University, Omaha, NE, United States*
[16] *Department of Physics, Aligarh Muslim University, Aligarh, India*

[17] *Department of Physics, Pusan National University, Pusan, Republic of Korea*
[18] *Department of Physics, Sejong University, Seoul, Republic of Korea*
[19] *Department of Physics, University of California, Berkeley, CA, United States*
[20] *Department of Physics, University of Oslo, Oslo, Norway*
[21] *Department of Physics and Technology, University of Bergen, Bergen, Norway*
[22] *Dipartimento di Fisica dell'Università and Sezione INFN, Cagliari, Italy*
[23] *Dipartimento di Fisica dell'Università and Sezione INFN, Trieste, Italy*
[24] *Dipartimento di Fisica dell'Università and Sezione INFN, Turin, Italy*
[25] *Dipartimento di Fisica e Astronomia dell'Università and Sezione INFN, Bologna, Italy*
[26] *Dipartimento di Fisica e Astronomia dell'Università and Sezione INFN, Catania, Italy*
[27] *Dipartimento di Fisica e Astronomia dell'Università and Sezione INFN, Padova, Italy*
[28] *Dipartimento di Fisica e Nucleare e Teorica, Università di Pavia, Pavia, Italy*
[29] *Dipartimento di Fisica 'E.R. Caianiello' dell'Università and Gruppo Collegato INFN, Salerno, Italy*
[30] *Dipartimento DISAT del Politecnico and Sezione INFN, Turin, Italy*
[31] *Dipartimento di Scienze e Innovazione Tecnologica dell'Università del Piemonte Orientale and INFN Sezione di Torino, Alessandria, Italy*
[32] *Dipartimento di Scienze MIFT, Università di Messina, Messina, Italy*
[33] *Dipartimento Interateneo di Fisica 'M. Merlin' and Sezione INFN, Bari, Italy*
[34] *European Organization for Nuclear Research (CERN), Geneva, Switzerland*
[35] *Faculty of Electrical Engineering, Mechanical Engineering and Naval Architecture, University of Split, Split, Croatia*
[36] *Faculty of Engineering and Science, Western Norway University of Applied Sciences, Bergen, Norway*
[37] *Faculty of Nuclear Sciences and Physical Engineering, Czech Technical University in Prague, Prague, Czech Republic*
[38] *Faculty of Science, P.J. Šafárik University, Košice, Slovakia*
[39] *Frankfurt Institute for Advanced Studies, Johann Wolfgang Goethe-Universität Frankfurt, Frankfurt, Germany*
[40] *Fudan University, Shanghai, China*
[41] *Gangneung-Wonju National University, Gangneung, Republic of Korea*
[42] *Gauhati University, Department of Physics, Guwahati, India*
[43] *Helmholtz-Institut für Strahlen- und Kernphysik, Rheinische Friedrich-Wilhelms-Universität Bonn, Bonn, Germany*
[44] *Helsinki Institute of Physics (HIP), Helsinki, Finland*
[45] *High Energy Physics Group, Universidad Autónoma de Puebla, Puebla, Mexico*
[46] *Hiroshima University, Hiroshima, Japan*
[47] *Hochschule Worms, Zentrum für Technologietransfer und Telekommunikation (ZTT), Worms, Germany*
[48] *Horia Hulubei National Institute of Physics and Nuclear Engineering, Bucharest, Romania*
[49] *Indian Institute of Technology Bombay (IIT), Mumbai, India*
[50] *Indian Institute of Technology Indore, Indore, India*
[51] *Indonesian Institute of Sciences, Jakarta, Indonesia*
[52] *INFN, Laboratori Nazionali di Frascati, Frascati, Italy*
[53] *INFN, Sezione di Bari, Bari, Italy*
[54] *INFN, Sezione di Bologna, Bologna, Italy*
[55] *INFN, Sezione di Cagliari, Cagliari, Italy*
[56] *INFN, Sezione di Catania, Catania, Italy*
[57] *INFN, Sezione di Padova, Padova, Italy*
[58] *INFN, Sezione di Pavia, Pavia, Italy*
[59] *INFN, Sezione di Torino, Turin, Italy*
[60] *INFN, Sezione di Trieste, Trieste, Italy*
[61] *Inha University, Incheon, Republic of Korea*
[62] *Institute for Gravitational and Subatomic Physics (GRASP), Utrecht University/Nikhef, Utrecht, Netherlands*
[63] *Institute for Nuclear Research, Academy of Sciences, Moscow, Russia*
[64] *Institute of Experimental Physics, Slovak Academy of Sciences, Košice, Slovakia*
[65] *Institute of Physics, Homi Bhabha National Institute, Bhubaneswar, India*
[66] *Institute of Physics of the Czech Academy of Sciences, Prague, Czech Republic*
[67] *Institute of Space Science (ISS), Bucharest, Romania*
[68] *Institut für Kernphysik, Johann Wolfgang Goethe-Universität Frankfurt, Frankfurt, Germany*
[69] *Instituto de Ciencias Nucleares, Universidad Nacional Autónoma de México, Mexico City, Mexico*
[70] *Instituto de Física, Universidade Federal do Rio Grande do Sul (UFRGS), Porto Alegre, Brazil*
[71] *Instituto de Física, Universidad Nacional Autónoma de México, Mexico City, Mexico*
[72] *iThemba LABS, National Research Foundation, Somerset West, South Africa*
[73] *Jeonbuk National University, Jeonju, Republic of Korea*
[74] *Johann-Wolfgang-Goethe Universität Frankfurt Institut für Informatik, Fachbereich Informatik und Mathematik, Frankfurt, Germany*
[75] *Joint Institute for Nuclear Research (JINR), Dubna, Russia*
[76] *Korea Institute of Science and Technology Information, Daejeon, Republic of Korea*
[77] *KTO Karatay University, Konya, Turkey*
[78] *Laboratoire de Physique des 2 Infinis, Irène Joliot-Curie, Orsay, France*
[79] *Laboratoire de Physique Subatomique et de Cosmologie, Université Grenoble-Alpes, CNRS-IN2P3, Grenoble, France*
[80] *Lawrence Berkeley National Laboratory, Berkeley, CA, United States*
[81] *Lund University Department of Physics, Division of Particle Physics, Lund, Sweden*
[82] *Moscow Institute for Physics and Technology, Moscow, Russia*
[83] *Nagasaki Institute of Applied Science, Nagasaki, Japan*
[84] *Nara Women's University (NWU), Nara, Japan*
[85] *National and Kapodistrian University of Athens, School of Science, Department of Physics , Athens, Greece*
[86] *National Centre for Nuclear Research, Warsaw, Poland*
[87] *National Institute of Science Education and Research, Homi Bhabha National Institute, Jatni, India*
[88] *National Nuclear Research Center, Baku, Azerbaijan*
[89] *National Research Centre Kurchatov Institute, Moscow, Russia*
[90] *Niels Bohr Institute, University of Copenhagen, Copenhagen, Denmark*
[91] *Nikhef, National Institute for Subatomic Physics, Amsterdam, Netherlands*
[92] *NRC Kurchatov Institute IHEP, Protvino, Russia*
[93] *NRC «Kurchatov»Institute – ITEP, Moscow, Russia*
[94] *NRNU Moscow Engineering Physics Institute, Moscow, Russia*
[95] *Nuclear Physics Group, STFC Daresbury Laboratory, Daresbury, United Kingdom*
[96] *Nuclear Physics Institute of the Czech Academy of Sciences, Řež u Prahy, Czech Republic*

[97] *Oak Ridge National Laboratory, Oak Ridge, TN, United States*
[98] *Ohio State University, Columbus, OH, United States*
[99] *Petersburg Nuclear Physics Institute, Gatchina, Russia*
[100] *Physics Department, Faculty of Science, University of Zagreb, Zagreb, Croatia*
[101] *Physics Department, Panjab University, Chandigarh, India*
[102] *Physics Department, University of Jammu, Jammu, India*
[103] *Physics Department, University of Rajasthan, Jaipur, India*
[104] *Physikalisches Institut, Eberhard-Karls-Universität Tübingen, Tübingen, Germany*
[105] *Physikalisches Institut, Ruprecht-Karls-Universität Heidelberg, Heidelberg, Germany*
[106] *Physik Department, Technische Universität München, Munich, Germany*
[107] *Politecnico di Bari and Sezione INFN, Bari, Italy*
[108] *Research Division and ExtreMe Matter Institute EMMI, GSI Helmholtzzentrum für Schwerionenforschung GmbH, Darmstadt, Germany*
[109] *Russian Federal Nuclear Center (VNIIEF), Sarov, Russia*
[110] *Saha Institute of Nuclear Physics, Homi Bhabha National Institute, Kolkata, India*
[111] *School of Physics and Astronomy, University of Birmingham, Birmingham, United Kingdom*
[112] *Sección Física, Departamento de Ciencias, Pontificia Universidad Católica del Perú, Lima, Peru*
[113] *St. Petersburg State University, St. Petersburg, Russia*
[114] *Stefan Meyer Institut für Subatomare Physik (SMI), Vienna, Austria*
[115] *SUBATECH, IMT Atlantique, Université de Nantes, CNRS-IN2P3, Nantes, France*
[116] *Suranaree University of Technology, Nakhon Ratchasima, Thailand*
[117] *Technical University of Košice, Košice, Slovakia*
[118] *The Henryk Niewodniczanski Institute of Nuclear Physics, Polish Academy of Sciences, Cracow, Poland*
[119] *The University of Texas at Austin, Austin, TX, United States*
[120] *Universidad Autónoma de Sinaloa, Culiacán, Mexico*
[121] *Universidade de São Paulo (USP), São Paulo, Brazil*
[122] *Universidade Estadual de Campinas (UNICAMP), Campinas, Brazil*
[123] *Universidade Federal do ABC, Santo Andre, Brazil*
[124] *University of Cape Town, Cape Town, South Africa*
[125] *University of Houston, Houston, TX, United States*
[126] *University of Jyväskylä, Jyväskylä, Finland*
[127] *University of Kansas, Lawrence, KS, United States*
[128] *University of Liverpool, Liverpool, United Kingdom*
[129] *University of Science and Technology of China, Hefei, China*
[130] *University of South-Eastern Norway, Tonsberg, Norway*
[131] *University of Tennessee, Knoxville, TN, United States*
[132] *University of the Witwatersrand, Johannesburg, South Africa*
[133] *University of Tokyo, Tokyo, Japan*
[134] *University of Tsukuba, Tsukuba, Japan*
[135] *University Politehnica of Bucharest, Bucharest, Romania*
[136] *Université Clermont Auvergne, CNRS/IN2P3, LPC, Clermont-Ferrand, France*
[137] *Université de Lyon, CNRS/IN2P3, Institut de Physique des 2 Infinis de Lyon, Lyon, France*
[138] *Université de Strasbourg, CNRS, IPHC UMR 7178, F-67000 Strasbourg, France*
[139] *Université Paris-Saclay Centre d'Etudes de Saclay (CEA), IRFU, Départment de Physique Nucléaire (DPhN), Saclay, France*
[140] *Università degli Studi di Foggia, Foggia, Italy*
[141] *Università di Brescia, Brescia, Italy*
[142] *Variable Energy Cyclotron Centre, Homi Bhabha National Institute, Kolkata, India*
[143] *Warsaw University of Technology, Warsaw, Poland*
[144] *Wayne State University, Detroit, MI, United States*
[145] *Westfälische Wilhelms-Universität Münster, Institut für Kernphysik, Münster, Germany*
[146] *Wigner Research Centre for Physics, Budapest, Hungary*
[147] *Yale University, New Haven, CT, United States*
[148] *Yonsei University, Seoul, Republic of Korea*

[I] Deceased.
[II] Also at: Italian National Agency for New Technologies, Energy and Sustainable Economic Development (ENEA), Bologna, Italy.
[III] Also at: Dipartimento DET del Politecnico di Torino, Turin, Italy.
[IV] Also at: M.V. Lomonosov Moscow State University, D.V. Skobeltsyn Institute of Nuclear, Physics, Moscow, Russia.
[V] Also at: Department of Applied Physics, Aligarh Muslim University, Aligarh, India.
[VI] Also at: Institute of Theoretical Physics, University of Wroclaw, Poland.
[VII] Also at: University of Kansas, Lawrence, Kansas, United States.